

Environmental Science and Engineering

Sijing Wang
Runqiu Huang
Rafiq Azzam
Vassilis P. Marinos *Editors*

Engineering Geology for a Habitable Earth: IAEG XIV Congress 2023 Proceedings, Chengdu, China

Volume 2: Geohazard Mechanisms, Risk
Assessment and Control, Monitoring
and Early Warning

 Springer

Environmental Science and Engineering

Series Editors

Ulrich Förstner, Buchholz, Germany

Wim H. Rulkens, Department of Environmental Technology, Wageningen,
The Netherlands

The ultimate goal of this series is to contribute to the protection of our environment, which calls for both profound research and the ongoing development of solutions and measurements by experts in the field. Accordingly, the series promotes not only a deeper understanding of environmental processes and the evaluation of management strategies, but also design and technology aimed at improving environmental quality. Books focusing on the former are published in the subseries Environmental Science, those focusing on the latter in the subseries Environmental Engineering.

Sijing Wang · Runqiu Huang · Rafiq Azzam ·
Vassilis P. Marinou
Editors

Engineering Geology
for a Habitable Earth: IAEG
XIV Congress 2023
Proceedings, Chengdu, China

Volume 2: Geohazard Mechanisms, Risk
Assessment and Control, Monitoring
and Early Warning

 Springer

Editors

Sijing Wang
Department of Hydraulic Engineering
Tsinghua University
Beijing, China

Runqiu Huang
Chengdu University of Technology
Chengdu, Sichuan, China

Rafiq Azzam
Department of Engineering Geology
and Hydrogeology
RWTH Aachen University
Aachen, Germany

Vassilis P. Marinos
School of Civil Engineering
National Technical University of Athens
Zografou, Greece

ISSN 1863-5520 ISSN 1863-5539 (electronic)
Environmental Science and Engineering
ISBN 978-981-99-9060-3 ISBN 978-981-99-9061-0 (eBook)
<https://doi.org/10.1007/978-981-99-9061-0>

© The Editor(s) (if applicable) and The Author(s), under exclusive license to Springer Nature Singapore Pte Ltd. 2024

This work is subject to copyright. All rights are solely and exclusively licensed by the Publisher, whether the whole or part of the material is concerned, specifically the rights of translation, reprinting, reuse of illustrations, recitation, broadcasting, reproduction on microfilms or in any other physical way, and transmission or information storage and retrieval, electronic adaptation, computer software, or by similar or dissimilar methodology now known or hereafter developed.

The use of general descriptive names, registered names, trademarks, service marks, etc. in this publication does not imply, even in the absence of a specific statement, that such names are exempt from the relevant protective laws and regulations and therefore free for general use.

The publisher, the authors and the editors are safe to assume that the advice and information in this book are believed to be true and accurate at the date of publication. Neither the publisher nor the authors or the editors give a warranty, expressed or implied, with respect to the material contained herein or for any errors or omissions that may have been made. The publisher remains neutral with regard to jurisdictional claims in published maps and institutional affiliations.

This Springer imprint is published by the registered company Springer Nature Singapore Pte Ltd. The registered company address is: 152 Beach Road, #21-01/04 Gateway East, Singapore 189721, Singapore

If disposing of this product, please recycle the paper.

Academic Committee

Academic Committee Chairs

Sijing Wang
Runqiu Huang

Academic Committee Members

Anthony Bowden
Bin Shi
Bo An-Jang
Carlos Delgado
Charles W. W. Ng
Chungsik Yoo
Defang Kong
Dingcheng Huang
Faquan Wu
Fawu Wang
Helen Reeves
Hengxing Lan
Hsein Juang
Huiming Tang
Janusz Wasowski
Jean Hutchinson
Jean-Alain Fleurisson
Jian Yang
Jianbing Peng
Jianmin Zhang
Jianxin Hua

Jinxu Yan
John Ludden
Julien Cohen-Waeber
Kyoji Sassa
Lansheng Wang
Manchao He
Martin Culshaw
Moshood Niya Tijani
Nicola Casagli
Niek Rengers
Peng Cui
Qing Wang
Rafiq Azzam
Ranjan Kumar Dahal
Resat Ulusay
Ricardo Oliveira
Roger Frank
Scott F. Burns
Shitian Wang
Shutao Yang
Vassilis Marinos
Victor Manuel Hernandez Madrigal
Wei Wu
Wei Zhang
Xiao Li
Xiating Feng
Yong-Seok Seo
Yueping Yin
Yusheng Gao
Zelian Chen
Zuyu Chen

Organizing Committee Chairs

Qiang Xu
Qiangbing Huang
Shengwen Qi
Xiangjun Pei
Xiaoqing Chen
Yuyong Jiao
Xuanmei Fan

Organizing Committee Members

Chaojun Ouyang

Chaosheng Tang

Jianjun Zhao

Liangqing Wang

Ning Liang

Wen Zhang

Yuhuan Song

Preface

The XIV Congress of the International Association for Engineering Geology and the Environment (XIV IAEG Congress 2023) was successfully held in Chengdu, China, from September 21 to 27, 2023. Focusing on the main theme “Engineering Geology for a Habitable Earth,” researchers and practitioners worldwide from academia, industry, and government have joined us in this prestigious event. Based on the topics discussed at the congress, the proceedings are organized into six volumes as follows:

- Volume 1: Engineering Geomechanics of Rock and Soil Masses
- Volume 2: Geohazard Mechanisms, Risk Assessment and Control, Monitoring and Early Warning
- Volume 3: Active Tectonics, Geomorphology, Climate and Geoenvironmental Engineering Geology
- Volume 4: Technological Innovation and Applied for Engineering Geology
- Volume 5: Megacity Development and Preservation of Cultural Heritage Engineering Geology
- Volume 6: Marine and Deep Earth Engineering Geology.

Meanwhile, on behalf of the organizing committee, we would also like to express our deepest appreciation to the technical program committee members, reviewers, session chairs, and volunteers for their strong support for congress.

Last but not least, our gratitude also goes to the editors and press for their great support to the congress.

September 2023

IAEG XIV Congress 2023 Organizing Committee

Contents

1	Rock Avalanches’ Morphological Classification: Important Tool for Risk Assessment	1
	Alexander Strom	
2	Enhancing Spectral Clustering Performance Using Self-Supervised Support Vector Machines for Regional Landslide Risk Assessment Visualization: A Case Study in Han-Yuan County, Ya’an City	13
	Yuting Ma, Mei Han, Shiyuan Zeng, Huijing Li, and Zihao Gao	
3	A Comprehensive Landslide Hazard Assessment Around Transmission Lines After the 2022 Ms6.8 Luding Earthquake, China	29
	Xiao Ling, Jianao Cai, Liang Zhang, and Dongping Ming	
4	Research on Intelligent Recognition Algorithms for Common Subgrade Diseases Based on Radar Images	39
	Mingzhou Bai, Yanli Qi, Jiazhi Li, Zelin Li, Linlin Song, Lingkang Dai, and Gang Tian	
5	Stability Prediction of Rock Slope Based on Fuzzy Clustering GA-FNN Model	55
	Wenlian Zhang, Yudong Li, and Xiaoyun Sun	
6	Landslide Hazard Assessment in Trung Chai Commune, Sapa, Vietnam Using Frequency Ratio Method and Scoops3D	69
	Binh Van Duong, Igor Konstantinovich Fomenko, Dang Hong Vu, Kien Trung Nguyen, and Oleg Vladimirovich Zerkal	
7	Research on Prediction and Prevention of Nonuniform Deformation in Unsymmetrical Loading Tunnel	85
	Qiushi Liu, Bin Shao, Bo Wang, Wenqing Zhang, Zhanying Ju, Xinmin Ma, and Peng Wang	

8 Investigation of Dynamic Fragmentation Mechanism of Granular Column Collapse Via Discrete Element Analyses 99
Wenbin Chang, Aiguo Xing, and Kaiping Jin

9 An Improved Bond-Based Smoothed Particle Hydrodynamics for Simulating Progressive Failure of Rock Slope Under Seismic Conditions 117
Chengzhi Xia, Zhenming Shi, and Huanjia Kou

10 Numerical Investigation of Influence of Low Ice Friction on Mobility of Rock-Ice Avalanches 131
Yuhao Ren, Qingqing Yang, Fei Cai, and Zhiman Su

11 Research on Radar Forward Modeling for Detecting Urban Road Subgrade Disease Based on Radar 143
Dayong Wang, Yanli Qi, Mingzhou Bai, Zelin Li, Linlin Song, and Gang Tian

12 Causes and Damage of the 2020 Periglacial Debris Flows at Zelunglung Catchment in the Eastern Syntaxis of Himalaya 161
Hao Li, Kaiheng Hu, Xiaopeng Zhang, Shuang Liu, and Li Wei

13 Energy Dissipation Effect of Different Structures on Debris Flow 173
Bingtao Han, Zhankui Liu, Yuxin Jie, and Jianbo Fei

14 Numerical Simulation of a Rainfall-Induced Debris Flow: A Case Study in Tianquan County, Southwest China 183
Ruichen Zhou, Xiewen Hu, Bo Liu, Kun He, Chuanjie Xi, and Guanglin Huang

15 Investigation and Analysis of “6.21” Debris Flow in Jiuzhaigou County, Sichuan Province 199
Li Ning, Zhao Boju, Chang Ming, Shu Zhile, and Bu Xianghang

16 A Study on the Relationship Between Building Damage and Shallow Subsurface Ground in the 2015 Nepal Gorkha Earthquake 217
Nobusuke Hasegawa, Pradhan Om, Atsushi Yatagai, and Nobuhiko Toyama

17 Study on Rockfall Simulation Method Using Discontinuous Deformation Analysis 229
Guichen Ma

18 Investigating Challenges and Countermeasures for the Yoshinogawa River Environment in Japan 239
Qinxue Wang, Tomohiro Okadera, and Satoshi Kameyama

19	Estimation of Slip Surfaces Using the Results of Groundwater Logging in Fracture Zone Landslides	253
	Tsunataka Furuya and Jingcai Jiang	
20	Detection of Deep-Seated Gravitational Slope Deformations by Aerial Photo Interpretation and Statistical Analysis in an Accretionary Complex in Japan	263
	Teruyuki Kikuchi and Satoshi Nishiyama	
21	Response of Groundwater to Rainfall and the Recession Constant of Antecedent Precipitation in a Slope with Residual Soil	279
	Yukai Fu, Chunli Chen, Chenxing Wang, Tonglu Li, Zhongjie Fan, and He Liu	
22	A New Simulation Tool on Rockfall Fragmentation-Movement-Deposition Process	301
	Huang Jian, Wang Hao, Huang Xiang, Yuan Jingqing, and He Zicheng	
23	Comparison Study of Typical Landslides in Hong Kong and Shenzhen	319
	Aiguo Li, Weiqiang Feng, Zhongqi Yue, George Tham, and C. F. Lee	
24	Design and Application of a Flexible Enclosure for Seasonally Saline Frozen Areas in Airports	335
	Shuang Wang, Rui Wang, Hong Qin, Fumin Shu, and Biao Yang	
25	Mechanism and Structural Evidence of Interlayered Rock Slope Failures	349
	Mian Sohail Akram and Luqman Ahmed	
26	Engineering Geo-mechanics System for Coal and Gas Outbursts	359
	Xubiao Deng, Yanjie Hou, and Huaichang Yu	
27	Insights into a Large-Prone Area in the Eastern Margin of the Tibetan Plateau, China—A Case Study Along the Danba Reach of the Dadu River	383
	Yunsheng Wang, Liang Song, Ruibin Kou, Shicheng Liu, Tao Tang, Zhuo Feng, and Mingbin Zhan	
28	Critical Physical and Hydraulic Condition for Fine Grains Migration, Deposition and Self-dredging in Seepage Erosion of Gravel Soil	397
	Jiazhan Ren, Hui Dong, Fengming Tan, and Lei Wen	

29 Stability of Coal Pillars and Backfill Due to Intermittent Cut-and-Fill Mining Under Loose Aquifer 413
 Jiawei Liu, Zhenyu Yin, and Yingzhi Xia

30 Geological Hazard Risk Assessment of Landslide Geological Hazards in the Gushan Navigation and Hydropower Hub Reservoir Area 429
 Minhao Hu, Kunsheng Hu, Qiguo Wang, and Yi Hu

31 Integration of Passive Seismic Techniques to Investigate the Landslide Dam Generated by the Yang Jia Gou Rock Avalanche (Sichuan–China) 445
 Paola Capone, Vincenzo Del Gaudio, Janusz Wasowski, and Wei Hu

32 Identifying the Potential Landslides Along Dube Highway (Guangxi, China) in Dense Vegetation Environment by Time Series InSAR 457
 Xianlin Liu, Tao Yin, Youdong Chen, Yu Shao, and Keren Dai

33 Early Identification, Monitoring and Warning of Landslide Hazard in Northeast Sichuan Based on Integrated Remote Sensing Technology 465
 Peng He, Zhaocheng Guo, Hong Chen, Genhou Wang, and Haochen Wang

34 Real-Time Intelligent Monitoring of Rockfall in the Complex Environment 477
 Juan Liu, Hui Chen, and Ying Hu

35 Research on the Application of InSAR Technology for the Recognition of the Potential Danger of Suspected Geological Hazards 489
 Zhimin Feng, Haiqiang Xin, Yong Wang, Hairong Liu, and Shanqing Zhang

36 Potential Geohazards Identification and Deformation Monitoring by Time-Series InSAR Along Anhui Ningwu Expressway 505
 Dongsheng Qian, Hongxiang Wang, Xuewen Huang, Xiaoyong Li, Xiangsheng Liu, Lei Zhang, Yu Wang, Fanfan Li, and Jiahong Zhong

37 Failure Mode of Steep Bedding Slopes Undergoing Strong Earthquake 515
 Longqi Li, Kang Xie, and Nengpan Ju

38 Permanent Displacement of Slopes Considering Horizontal and Vertical Ground Motions Based on the Tensile-Shear Sliding Mode 527
 Xiao Cheng, Lianheng Zhao, Xinyan Peng, Dejian Li, Baofeng Di, and Yingbin Zhang

39 System Reliability Analysis of Geosynthetic-Reinforced Soil Slopes Under Seismic Conditions 545
 Rui Sun, Jianfeng Chen, Ming Peng, Ning Bao, and Hui Qi

40 Study on Development Stage and Evolution of Landslide in Wide Fracture Zone of Anninghe Active Fault 557
 Bin Liu, HongFu Zhou, Ming Liu, Su Zhang, Min You, and XiaoBo Ma

41 Monitoring Spatial–temporal Seismic Velocity Changes and Microstructural Changes on Rock Slope Associated with the M 6.8 Luding Earthquake 571
 Zhengran He, Li Zhao, and Fan Xie

42 Determination of Crucial Shear Parameters in Highly Landslide Prone Tropical Soils in Bello Oriente, Medellín, Colombia 583
 Tamara Breuninger, Bettina Menschik, Moritz Gamperl, and Kurosch Thuro

43 Post-wildfire Landslide Engineering: Hazard Assessment to Mitigation in the Cameron Peak Wildfire, Colorado, USA 593
 Thad Wasklewicz, Richard Guthrie, Paul Eickenberg, and Benjamin Kramka

44 Landslide Susceptibility in the Turkish Northwesternmost Sector: Distinctive Patterns of Inactive and Active Landslides 613
 Marco Loche, Hakan Tanyas, Gianvito Scaringi, Tolga Gorum, and Luigi Lombardo

45 Movement Process Analysis of Long-Runout Guanling Landslide in Guizhou, China 629
 Shunbo Zhang, Wenbing Shi, Xiongwu Peng, and Xiaoming Wang

46 Reinforced Slope with Micropiles Based on Centrifugal Simulation Test 649
 Yulin Xu, Dongdong Wu, and Dongpo Wang

47 Evaluating Dark Fiber Distributed Acoustic and Strain Sensing for Shallow Ground Movement Monitoring: A Field Trial 665
 Cheng-Cheng Zhang and Bin Shi

48 A Case Study of Automatically Monitoring System Experiment for Landslide Within Tianfu New District in Chengdu 675
Hu Depan, Wang Xuben, Luo Yongkang, Shi Lily, and Yang Huajin

49 A Practical Method to Predict the Occurrence Time of Storm-Induced Shallow Landslide Considering the Underlying Impermeable Bedrock 683
Li-Ming Zhang, Qing Lü, Jun-Yu Wu, Chang-Gui Xiao, Zheng-Hua Liu, and Xing-Hua Xu

50 Estimation of Seismic Earth Pressure Acting on Stabilizing Piles in Sandy Slopes Considering Soil Arching Effect 699
Ning Bao, Jianfeng Chen, and Rui Sun

51 Experimental Investigation on Impact Force of Dry Granular Flows on a Rigid Retaining Wall 713
Xiaoyi Fan, Yuanjun Jiang, Haonan Liu, and Huan Liu

52 Sliding Tbilisi: Why Georgia’s Capital is Haunted by Multiple Landslides 729
Klaus Keilig, Peter Neumann, Markus Bauer, Kurosch Thuro, and Zurab Menabde

53 Experimental Investigation and Numerical Simulation on Progressive Failure of Landslide Under Different Rainfall Conditions 743
Ni Jiji, Huang Yongliang, Sha Peng, and Liu Dongyan

54 The Occurrence of a Rainfall-Induced Catastrophic Landslide in a Soil and Rock-Like Stratum in Southwest China 761
Leilei Jin, Zhengfeng Chen, Wenxi Fu, Cheng Zhou, Bingshuang Ye, and Rui Qian

55 Various Applications of Developed DDA-SPH Method to Coupling Problems Involved in Geological Disasters 785
Xinyan Peng, Xiao Cheng, Pengcheng Yu, Baofeng Di, Yingbin Zhang, and Lu Zheng

56 Numerical Simulation of Crack Propagation in Jointed Rock Mass Based on an Enhanced SPH Method 799
Guangyin Lu, Chuanyi Tao, and Chengzhi Xia

57 Strength Characteristics of Ili Loess and Its Landslide Numerical Simulation 817
Boyu Gao, Zhijun Zhou, Yubo Ren, Jiayan Yi, and Zhongtong Sui

58 Mechanisms of Reservoir Impoundment-Induced Large Deformation of the Guobu Slope at the Laxiwa Hydropower Station, China: Preliminary Insights from Remote Sensing and Numerical Modelling 835
Moritz Lesche, Liang Wang, Andrea Manconi, Simon Loew, Qiang Yang, Yaoru Liu, and Qinghua Lei

Chapter 1

Rock Avalanches' Morphological Classification: Important Tool for Risk Assessment



Alexander Strom

Abstract Well-grounded and timely assessment of risks provided by hazardous phenomena in mountainous regions is an important factor of their sustainable development. Rock avalanches are among most critical due to large volumes, extreme mobility, ability to block river valleys. Assessment of risk produced by rock avalanches that will occur in such regions in future inevitably, requires prediction of the exposure that can be treated both directly—as size and shape of the area that might be affected by moving debris, and indirectly—by estimating height and shape of natural dam that could be formed in narrow valley, that predetermine magnitude of inundation and of the potential outburst flood. Such assessment can be performed using statistical relationships between initial slope failure parameters—volume and slope height, and resultant parameters –runout and affected area, derived for rock avalanches of different types. Their morphological classification takes into account the confinement conditions, debris distribution along travel path, directivity of debris motion. Further division within the selected types considers additional morphological and geotechnical factors such as shape of the deposits in plan view, interaction of rapidly moving rock avalanche debris with substrate and with obstacles. Future efforts should be concentrated on compilation of the uniform worldwide rock avalanches database allowing statistically representative analysis for each type and subtype selected according to the proposed classification system.

Keywords Rock avalanche · Classification · Morphology · Risk assessment

A. Strom (✉)

Research Institute of Energy Structures—Branch of JSC, Hydroproject Institute, Moscow, Russia
e-mail: strom.alexandr@yandex.ru

1.1 Introduction

Sustainable development of mountainous regions, prone to various hazardous phenomena endangering population, industrial objects and infrastructure is impossible without well-grounded and timely assessment of associated risks. Those provided by rock avalanches are among most critical due to their large volumes, extreme mobility, ability to block river valleys. Besides, being closely associated with earthquakes and climatic events such as global warming, rock avalanches can increase severity of their consequences significantly.

It is obvious that such large-scale rock slope failures that had occurred in the past repeatedly almost in all mountain systems, will inevitably occur in future. Where, how large, and when—is a challenging problem, requiring both regional and site-specific studies and monitoring. However, if the potentially unstable high slope is identified, the next step is to estimate size and shape of the area at a slope foot that might be affected to assess the exposure defined as “People, property, systems, or other elements present in hazard zones that are thereby exposed to potential losses” (Corominas et al. 2015). In this context the “hazard zone” can be treated either directly—as size and shape of the area that might be affected by collapsing slope and moving debris, or indirectly—by estimating height and shape of natural dam that could be formed in narrow valley, that, in turn, predetermine magnitude of inundation and of the potential outburst flood.

Such assessment can be based on two main approaches: (1) the numerical modelling, and (2) use of the statistical relationships between initial slope failure parameters—volume and slope height, and resultant parameters—runout and affected area (Iverson 2006). The first one is rather laborious and requires variable input data that, often, can be hardly obtained. Use of the statistical relationships, in contrast, is quite simple. On the other hand, it is efficient, if type of the anticipated rock avalanche corresponds well to rock avalanches’ type for which the utilized relationship(s) has been derived. It determines importance of detailed classification of this natural phenomenon.

Rock avalanches always originate as rock slides or different types—planar, wedge, rotational, irregular, compound (Hungri et al. 2014). It should be pointed out that transition from the initial sliding to the (predominantly) dry granular flow typical of rock avalanches might occur quite fast, that can be illustrated by several videos available, for example, in Landslide blog (D. Pettly, <https://blogs.agu.org/landslide-blog/>). Types of rock slides converting into rock avalanches listed in Table 1 in Strom et al. (2021) can be complemented by spreads that are rather common in the Alpine belt (Strom et al. 2021) and can be exemplified by numerous rock avalanches that collapsed from the ca. 1 km high southern cliff of the Caucasian Rocky Range composed of Upper Jurassic limestone underlain by clayey easily deformable Middle Jurassic flysch (Strom 2004).

After rock slides of all types mentioned above transformation into granular flow—rock avalanche—the latter interact with the relief of the travel path and substrate over which it moves and, thus, can behave in different ways forming deposits with quite

variable shapes. Thus, rock avalanches can be divided in several types based on different classification criteria. Three of them: (i) Confinement; (ii) Debris distribution along its travel path; (iii) Debris motion directivity, can be considered as most important.

1.2 Classification Based on the Confinement Conditions

The first classification criterion—the confinement conditions allowing selection of unconfined, frontally confined and laterally confined types is most obvious (Fig. 1.1). Further subdivision is based on the degree of freedom of debris distribution immanent for each of these tree basic types.

The degree of freedom of the laterally confined rock avalanches is minimal—they can move ahead only (how far ahead—is another problem requiring special analysis) and, thus, their subdivision is useless. In contrast, debris of the unconfined and frontally confined rock avalanches can spread both ahead (upslope in case of frontal confinement) and sidewise, allowing selection of several morphological subtypes. Unconfined roc avalanches are divided into three subtypes—“mono-directional”, “fan-shaped” and “isometric” (Fig. 1.2). Frontally confined—into “compact” and “widened” subtypes (Fig. 1.3).

Such subdivision is directly related to exposure assessment. Indeed, mono-directional rock avalanche that moves strictly forward, forming a tongue of debris whose width is more or less constant and almost equal to the headscarp base width (Figs. 1.1a, 1.2a), might have longer runout than fan-shaped or isometric rock avalanche that spreads sidewise significantly. The latter, however, can cover larger area, providing larger exposure, though may be not so distant from the slope base.

Somehow similar is the behavior of rock avalanche bodies that move across relatively narrow valleys whose opposite slopes provide frontal confinement. They

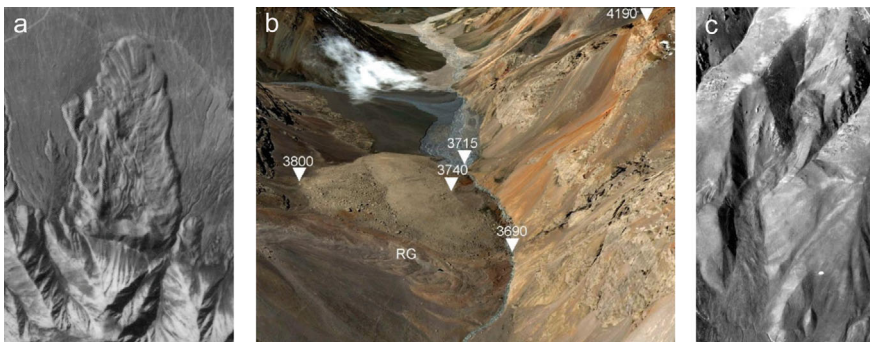


Fig. 1.1 Types of rock avalanches from Central Tien Shan in different confinement conditions. **a** 5-km long unconfined Chaarash-3 RA; **b** frontally confined Kainar RA at the foot of 500 m high slope; **c** 2.5-km long laterally confined Chongsu RA

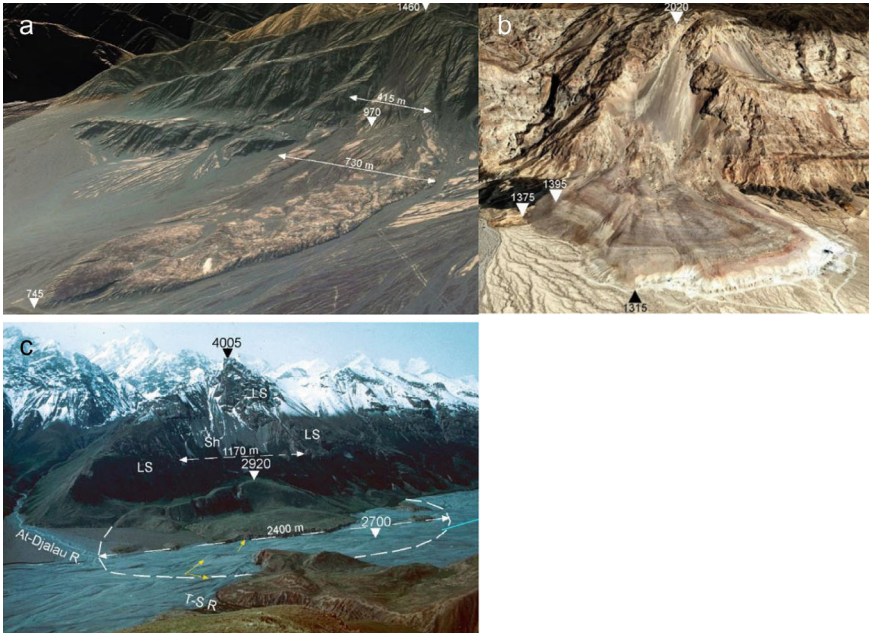


Fig. 1.2 Types of unconfined rock avalanches. **a** Mono-directional RA in Chinese Tien Shan; **b** fan-shaped RA in Chinese Tien Shan; **c** isometric At-Djailau RA in Kyrgyz Tien Shan

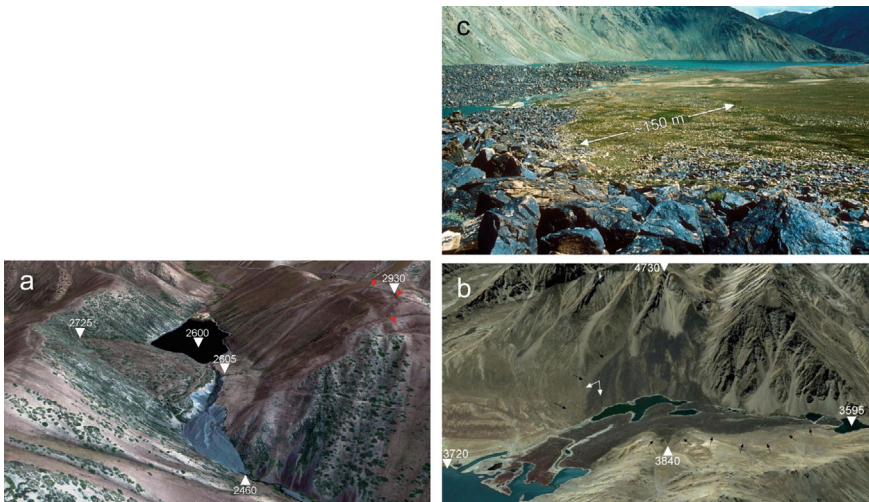


Fig. 1.3 Types of frontally confined rock avalanches. **a** Compact Chong-Tash RA rock avalanche with 120 m runup, up to 2725 m, Central Tien Shan, Kyrgyzstan. Red triangles mark headscarp; **b** widened Yashilkul RA, Central Pamir, Tajikistan. Black arrows mark the outer boundary of rock avalanche whose frontal and right-side zone is composed of morain material pushed out by gneiss boulders (see photograph in “c” made from the point marked in “b” by white double-headed arrow)



Fig. 1.4 Frontally confined widened Karasu Lake RA of the secondary type described hereafter, Central Tien Shan, Kyrgyzstan. Yellow dashed line—boundary of the dam body; yellow triangles mark the so-called secondary scar; T—trimline of the secondary rock avalanche

also can move mainly forward, forming compact and relatively high natural dams (Figs. 1.1b, 1.3a), or can spread along the blocked valley, sometimes both up- and down-valley (Fig. 1.3b), or just down-valley (Fig. 1.4). It is obvious that such spreading should reduce dams' height and, consequently, possible volume of the stored water that can be released afterward during dam breach.

If such spreading is more or less uniform it decreases seepage gradient influencing dam's erosion and piping resistance. Such effect, along with high permeability of coarse blocky carapace with large voids that is well visible in Fig. 1.3c, supports gradual outflow from dammed lakes increasing their longevity and decreasing probability of catastrophic dam breach and outburst flood (Fan et al. 2020, 2021). On the other hand, the along-valley debris spreading can reduce thickness of the upper part of the dam that can be exemplified by the Karasu Lake Rock avalanche shown in Fig. 1.4. Such effect can be, more likely, considered as negative, as far as it increases probability of the destruction of the dams' crest. Such interplay of "positive" and "negative" effects should be analyzed individually at each particular case.

1.3 Classification Based on Debris Distribution Along Its Travel Path

Another important rock avalanches’ classification criterion is debris distribution along its travel path (Fig. 1.5). It characterizes rock avalanche morphology regardless of the confinement conditions and of the relief of the transition and deposition area. Three main types– “primary”, “jumping”, and “secondary” rock avalanches are selected (see Fig. 1.1) (Strom et al. 2021; Strom and Abdrakhmatov 2018).

Those ascribed to the primary type are characterized by debris accumulation at the distal part of the travel path. For unconfined and laterally confined cases (Fig. 1.5-1a) it looks as if almost all debris “flowed down” as far as possible. Primary frontally confined rock avalanches (Fig. 1.5-1b) are characterized by the significant

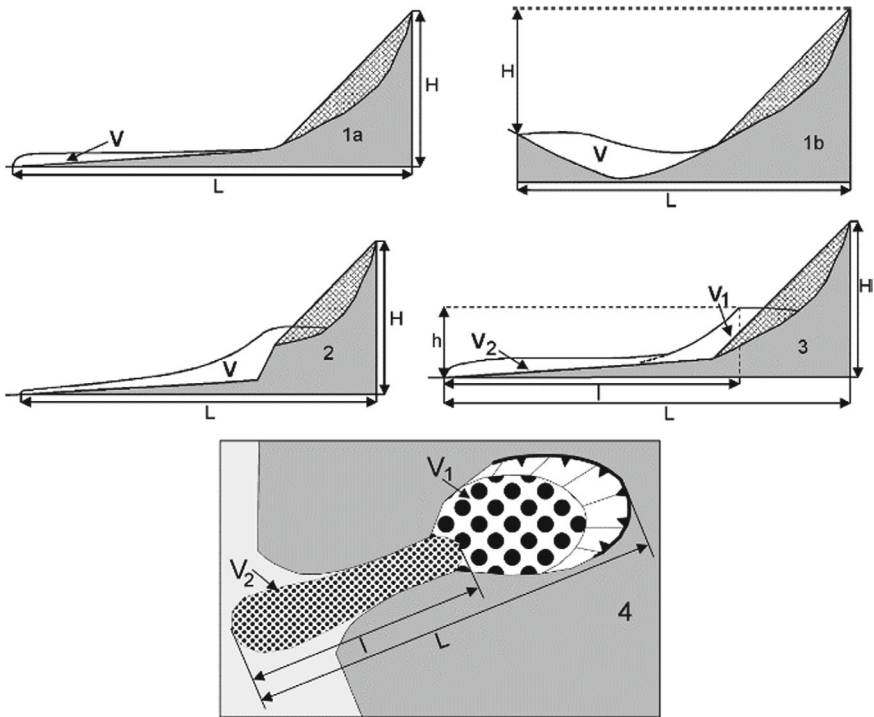


Fig. 1.5 Rock avalanche types based on the along-way debris distribution. 1—primary rock avalanche: 1a—in unconfined or laterally confined conditions, 1b—in frontally confined conditions; 2—jumping rock avalanche; 3, 4—secondary rock avalanches of the “classical” and the “bottleneck” subtypes correspondingly. H—height drop (vertical distance between the headscarp crown and the deposits tip); h—that of the secondary rock avalanche; L—runout; l—secondary rock avalanche runout; V—entire volume, V₁—volume of the compact part of the secondary rock avalanche, V₂—that of its avalanche-like part. (After Strom and Abdrakhmatov 2018, with permission from Elsevier)

runup (Figs. 1.1b, 1.3a), so that the lowermost part of the dam's crest is close to the headscarp base.

Rock avalanches of the jumping (Fig. 1.5-2) and secondary (Fig. 1.5-3, 4) types are characterized by distinct bipartition of their bodies with compact accumulation at the headscarp base and elongated mobile part. They can be distinguished, further, by the style of the transition from compact to mobile part. For jumping rock avalanches that really jumped as from the ski-jump (their sliding surface daylighted much above slope base) such transition is rather gradual, while secondary rock avalanches have either distinct circus-like depression on the slope of compact body raising above the mobile avalanche-like part (Fig. 1.5-3), or the latter passes through sharp valley constriction (Fig. 1.5-4).

Importance of this classification criterion for rock avalanche hazard and risk assessment is determined by several factors. First, by the excessive mobility of secondary rock avalanches that provide longer runout of their mobile parts than average runout of other types of rock avalanches of the similar volume (Strom and Abdrakhmatov 2018). Second—by the specific shape of the primary rock avalanches in frontally confined conditions that can be exemplified by cases shown in Figs. 1.1b and 1.3a. As far as large portion of debris raised on the opposite valley slopes, it reduced the effective height of rock avalanche dams—their minimal crest level. It can be compared with the longitudinal profile of the Karasu Lake dam (Fig. 1.4) that is much more constant. Such position of the lowermost point of the dam's crest limits lake depth. Besides, proximal parts of such natural dams are often composed of loose material accumulated there after main slope failure and, usually, more vulnerable for rapid erosion in case of overtopping. And the last, but not the list, is the possibility of drastic change of the direction of secondary and jumping rock avalanches debris motion, impossible for primary rock avalanches, that will be described in the next section.

1.4 Classification Based on Debris Motion Directivity

The mobile parts of secondary and jumping rock avalanches can move either in the same direction as the initial slope failure ("unidirectional" subtype), or can change direction of their motion, sometimes up to 90° ("deflected" subtype). It is especially impressive at secondary rock avalanches. In the first case distinct secondary scar that marks the transition from the initial slope failure and ejection of the mobile part, is well visible on the frontal slope of compact accumulation (Fig. 1.1c). In the second case, secondary scar appears on the downstream slope of the dam body (Figs. 1.4, 1.6).

Such deflection requires significant transformation of the momentum, gained during the initial downslope descent. Since momentum is a vector value, here its directivity is changing indicating momentum transfer. Possibility of a drastic change of rock avalanche debris motion must be taken into account for hazard and risk assessment since the deflected rock avalanche can affect objects that otherwise can



Fig. 1.6 Southern Karakungey secondary RA with almost 90° change of debris motion direction. Blue arrow—direction of the initial slope failure; green arrow—that of the secondary failure

be considered as safe, being located quite far from the area endangered by the initial slope failure. It could increase hazard produced by such rock avalanches significantly.

1.5 Interplay of Classification Criteria and Its Application

Three classification criteria described above can be combined in different ways. They can be considered independently, as in Sects. 1.2–1.4 (see also multilevel classification proposed in Strom et al. 2021), but, at the same time, all of them can be used as additional criteria allowing more detailed description of a particular case study as exemplified in Fig. 1.7. Selection of a certain order of the criteria used to describe and classify rock avalanches depend on the purpose and objectives of the study.

Specifically, the relationships between slope failure volume and height drop (slope height)—parameters characterizing initial state of the collapsing rock mass on the one hand, and rock avalanche runout and affected area on the other hand, were derived for samples selected according to confinement conditions (Shaller 1991; Nicoletti and Sorriso-Valvo 1991; Corominas 1996; Strom et al. 2019). Such approach is obvious since combining of all three types for runout analysis is meaningless, similarly to combining laterally confined and unconfined events to analyze area of the deposits. Separate analysis performed for Central Asian database provided quite high correlation coefficients ($R^2 > 0.9$) for some of these regressions (Strom and Abdrakhmatov 2018; Strom et al. 2019).

If main research interest is focused on hazards and risks associated with formation and evolution of rock avalanche dams, the priority should be also given to confinement since such dam can originate in frontally confined conditions mainly.

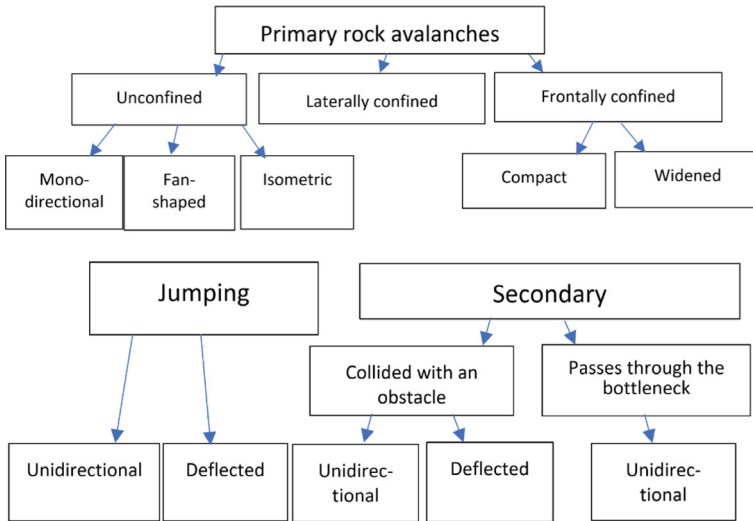


Fig. 1.7 Two variants of combination of rock avalanche classification criteria with the along-way debris distribution as a primary one

Debris motion directivity will be quite important for prediction of the exposure, especially if the collapsing rock mass is quite large and can collide with an opposite valley slope obliquely. It will be interesting to analyze in future, using larger database, how the behavior of debris depends on the collision angle.

But if we are most interested in mechanism of debris motion, it seems that here the priority should be given to the along-way debris distribution that allows classifying rock avalanches regardless both of the confinement conditions (compare cases 1a and 1b in Fig. 1.5) and of debris motion directivity. One more quiet promising research field is the analysis of factors governing different shapes of unconfined rock avalanches—why some of them moved just forward forming narrow tongues of debris, while other spread sidewise significantly. It can be hypothesized that such variability depends on the mechanical properties (shear strength) of the substrate at the base of moving rock avalanche (Grigorian 1979), but more field data and geotechnical tests are necessary to prove or disprove this assumption.

1.6 Conclusions: Future Research Directions

Classification presented herein in brief and its applications are based on the analysis of the Central Asian rockslide database mainly (Strom and Abdrakhmatov 2018). Despite large number of cases included in the database—ca. 1000, for about 600 of which various quantitative characteristics have been provided to date, it seems not to be large enough to perform statistical analysis of samples based more than

on one classification criterion. Further research program includes, first, quantitative characterization of the remaining Central Asian cases for which it has not been done yet; second, enlargement of the study area aimed to increase number of cases that can be ascribed to a particular type and subtype up to the amount suitable for regression analysis.

For this purpose, it will be interesting to combine several large regional databases (e.g., for Karakorum region, Hewitt 1988, 2011), but it requires careful comparison of terms and parameters, to be sure that values used in both (in all of them) describes similar characteristics.

Larger and statistically more representative samples considering several classification criteria will allow elaboration of more grounded relationships that can be used for rock avalanche hazard and risk assessment at those sites where large-scale rock slope failures can be anticipated. It will help to propose reasonable risk mitigation and, may be, hazard prevention measures to decision makers and local and/or regional or state authorities.

References

- Corominas J (1996) The angle of reach as a mobility index for small and large landslides. *Can Geotech J* 33:260–271
- Corominas J, Einstein H, Davis T, Strom A, Zuccaro G, Nadim F, Verdel T (2015) Glossary of terms on landslide hazard and risk. In: Lollino G et al (eds) *Engineering geology for society and territory*, pp 1775–1779. https://doi.org/10.1007/978-3-319-09057-3_314
- Fan X, Dufresne A, Subramanian SS, Strom A, Hermanns R, Tacconi Stefanelli C, Hewitt K, Yunus AP, Dunning S, Capra L, Geertsema M, Miller B, Casagli N, Jansen JD, Xu Q (2020) The formation and impact of landslide dams. *The formation and impact of landslide dams—State of the art. Earth Sci Rev.* <https://doi.org/10.1016/j.earscirev.2020.103116>
- Fan X, Dufresne A, Whiteley J, Yinus AP, Subramanian SS, Okeke CAU, Pánek T, Hermanns R, Ming P, Strom A, Havenith H-B, Dunning S, Wang G, Tacconi Stefanelli C (2021) Recent advances in landslide dam investigations and hazard assessment. *Earth Sci Rev*
- Grigorian SS (1979) The new friction law and the mechanism of large scale rock falls and landslides. *Sov Phys Dokl* 24:110–111
- Hewitt K (1988) Catastrophic landslide deposits in the Karakoram Himalaya. *Science* 242:64–67
- Hewitt K (2011) Rock avalanche dams on the trans Himalayan up-per indus streams: a survey of late quaternary events and hazard-related characteristics. In: Evans SG, Hermanns R, Strom AL, Scarascia-Mugnozza G (eds) *Natural and artificial rockslide dams. Lecture notes in earth sciences*. Springer, Heidelberg, pp 177–204
- Hung O, Leroueil S, Picarelli L (2014) Varnes classification of landslide types, an update. *Landslides* 11:167–194
- Iverson RM (2006) Forecasting runout of rock and debris avalanches. In: Evans SG et al (eds) *Landslides from Massive rock slope failure. NATO science series: IV: earth and environmental sciences*. Springer, New York, pp 197–209
- Nicoletti PG, Sorriso-Valvo M (1991) Geomorphic controls of the shape and mobility of rock avalanches. *Geol Soc Am Bull* 103:1365–1373
- Shaller PJ (1991) Analysis and implications of large martian and terrestrial landslides, Ph.D. Thesis, California Institute of Technology, p 569
- Strom AL (2004) Rock avalanches of the Ardon River valley at the southern foot of the Rocky Range, Northern Caucasus, North Ossetia. *Landslides* 1:237–241

- Strom A, Abdrakhmatov K (2018) Rockslides and rock avalanches of Central Asia: distribution, morphology, and internal structure. Elsevier, Amsterdam, p 449
- Strom A, Li L, Lan H (2019) Rock avalanche mobility: optimal characterization and the effects of confinement. *Landslides* 16:1437–1452
- Strom A (2021) Rock avalanches: basic characteristics and classification criteria. In: Vilimek V et al (eds) *Understanding and reducing landslide disaster risk*, vol 5. *Catastrophic landslides and frontiers of landslide science*. Springer, London, pp 3–23

Chapter 2

Enhancing Spectral Clustering Performance Using Self-Supervised Support Vector Machines for Regional Landslide Risk Assessment Visualization: A Case Study in Han-Yuan County, Ya'an City



Yuting Ma, Mei Han, Shiyuan Zeng, Huijing Li, and Zihao Gao

Abstract In this paper, A novel application, self-supervised support vector machine learning, is proposed to enhance the performance of an unsupervised spectral clustering model in regional landslide risk assessment visualization. Taking Han-Yuan County, Ya'an City, as the case study, we utilized spectral clustering to train the sample set and attained the optimal kernel function parameter value of 0.03, which was then applied to the total sample for classification prediction and an AUC value of 0.819 was achieved. To further improve the model performance, we applied self-supervised learning on the basis of the spectral clustering. After introducing this approach, the model performance was substantially improved, with an AUC value of 0.954, representing an increase of 13.5% compared to the unsupervised spectral clustering, and the calculation time was increased by only 0.017 s, which was negligible. The improved algorithm also produced a landslide susceptibility risk evaluation map for Han-Yuan County, Ya'an City, indicating that the high-risk area and the extremely high-risk area occupied 27.05% of the entire landslide, but accounted for 83% of the landslides, confirming the efficacy of this method in terms of enhancing the accuracy of spectral clustering.

Keywords Landslide risk assessment · Spectral clustering · Support vector machine · Susceptibility mapping

Y. Ma · M. Han (✉) · S. Zeng · H. Li
School of Mathematics, Southwest Jiaotong University, Chengdu 611756, China
e-mail: hanmei@home.swjtu.edu.cn

S. Zeng
e-mail: song_zeng@gtmc.com.cn

Z. Gao
Sichuan University of Science and Engineering, Zigong 643000, Sichuan, China

2.1 Introduction

In recent decades, the prevention and control of geological disasters such as collapses, landslides and debris flows has become an increasingly pressing public safety challenge for human survival and development, engineering economic construction, and even leisure and exploration activities (Yin et al. 2020; Wang et al. 2021; Qing and Shao 2022). Drawing on this concern, in 2022 Wang (2022) highlighted in several issues concerning geological disaster prevention and control, the need for the establishment and improvement of an information platform for such prevention and control, and the application of new technologies like 5G, IoT, big data, cloud computing, and AI to facilitate digitalization, networking, visualization, and intelligent management of “One Map”. This also requires the intelligent and visual risk assessment of landslides. In recent years, scholars at home and abroad have studied ways to realize such visualization of regional landslides risk assessment (Cai 2021; Chen et al. 2022; Frangov et al. 2017). However, an efficient, simple and accurate method remains an urgent problem to be solved.

The essence of research on landslide risk assessment lies in classification. Currently, this typically entails either deterministic or non-deterministic method (Xi et al. 2022). Deterministic methods evaluate the risk of landslide hazard by traditional mechanical calculation models, which are based on the principle and physical mechanism of landslide occurrence (Jiang et al. 2017; Ramzani and Dehghan 2022; Xu et al. 2022). However, due to the clear physical meaning, high precision requirements for basic parameters, and difficulty in obtaining data associated with traditional physical models, they are best suited for the study of specific monomer landslides.

The non-deterministic approach to landslide risk assessment involves both qualitative and statistical analyses (Liu et al. 2022), with the former relying on knowledge-driven methods such as hierarchical analysis (Shao and Zheng 2018), fuzzy comprehensive evaluation (Wang et al. 2020), grey correlation analysis (Niu et al. 2019) and expert rating (Yan et al. 2015), and the latter on data-driven methods such as information content, artificial neural networks (Segoni 2018), monte Carlo simulations (Nayek 2021), logistic regression (Ou et al. 2021), support vector machines (Aslam et al. 2022), random forests (Aslam 2021) and clustering (Mao et al. 2021). While most data-driven methods require a large amount of data, clustering algorithms do not, allowing for rapid feature extraction. Over the past decades, a variety of clustering algorithms have been developed, from hierarchical clustering to K-means to EM and, more recently, spectral clustering (Garcia 2022; Garcia et al. 2022, 2023).

Nowadays, the spectral clustering algorithm is widely used in clustering applications due to its good performance. This algorithm transforms a clustering problem into a graph-cutting problem, and has been applied by Du et al. (2021). to characterize seafloor landslides, concluding that the input factor category could be appropriately simplified when data are insufficient. As an unsupervised learning algorithm, spectral clustering is based on graph abstraction, allowing for the clustering of data points by calculating the eigenvalues of the graph (Zong et al. 2022; Bai et al. 2021; Zhang

et al. 2019). Nevertheless, few studies have looked into its application in landslide risk assessment.

This paper introduces a novel application of SVMs wherein they are used to improve the performance of unsupervised spectral clustering. A self-supervised approach is then adopted to further enhance the accuracy of the model, which was applied to the case study of Han yuan County in Ya'an City. This qualitative approach helped to assess regional risks in a relatively short time and with limited resources. Additionally, it provided a new research idea for regional landslide risk assessment.

2.2 Description of the Study Area

In recent years, Han yuan County, located in the mountainous region of Ya'an City, China, has been heavily affected by landslides, resulting in significant economic losses and human casualties. The area is particularly prone to landslides due to its steep topography and high rainfall. Since the beginning of 2021, the county has experienced a series of severe landslides, with devastating effects. In March 2021, for example, a severe landslide occurred in Liu ping Township, Han yuan County, resulting in the collapse of a number of houses and the death of three people. In April 2021, another landslide occurred in Xin fa Township, Han yuan County, resulting in the destruction of two bridges and the death of four people. Such disasters have caused huge economic losses and displacement of local residents, and have raised growing concern over the vulnerability of the county to landslides (Tang et al. 2015). To mitigate the potential risks of landslides and to improve the safety of the local population, it is essential to strengthen the landslide risk assessment and mitigation measures in Han yuan County.

The present study was conducted in Han Yuan County, Ya'an City, China, bounded by latitudes $30^{\circ}30'N$ to $32^{\circ}14'N$ and longitudes $102^{\circ}33'E$ to $104^{\circ}40'E$ in the UTM Zone 50 N (Fig. 2.1). The study area covers an area of 2624 km². Rainfall in the area is concentrated in a single monsoonal season from June to September, with high intensity and wide areal coverage resulting in frequent flooding. To date, no studies have been conducted on landslides and related problems in this area, making this study an important baseline for landslide risk assessment in the region.

2.3 Data Sources and Processing

The selection of influencing factors for landslide risk assessment is a crucial basic step. Using independent data may introduce redundant information and generate noise, hindering the power of the model. Despite this, there is yet to be consensus on which conditions should be identified. In general, scholars suggest five broad categories for impact factors, namely geology, hydrology, land cover, geomorphology and others (Yu et al. 2014). For the purpose of this study, nine key conditioning factors